ISSN 0965-545X, Polymer Science, Ser A, 2006, Vol. 48, No. 9, pp. 951-960. © Pleiades Publishing, Inc., 2006. Published in Russian in Vysokomolekulyarnye Soedineniya, Ser. A, 2006, Vol. 48, No. 9, pp. 1628-1639.

Rheology and Fiber Degradation during Shear Flow of Carbon-Fiber-Reinforced Polypropylenes[1]

B. Hausnerova*, N. Honkova, A. Lengalova, T. Kitano, and P. Saha

Tomas Bata University in Zlín, Faculty of Technology, Polymer Centre, T.G. Masaryka 275, CZ-762 72 Zlín, Czech Republic
**e-mail: hausnerova@ft.utb.cz*

Abstract—The processing of fiber-reinforced thermoplastics is often accompanied by a significant fiber fracture. Therefore, it is important to assess the effect of processing variables on the extent of fiber damage occurring during product fabrication, such as extrusion or injection molding. The present paper discusses fiber damage caused by shear forces exerted on the composite by a molten matrix in both experimental and theoretical terms. The degradation process in carbon fiber-polypropylene composites is studied in a broad range of shear rates, although it occurs significantly only under high shearing in a capillary. Changes in fiber length and its distribution during the multi-flow through a capillary, as well as the materials' rheological properties found in research after shearing, are discussed and the results are compared with a model of fiber-length analysis for the mixing-regrinding process.

DOI: 10.1134/S0965545X06090100

[1] The text was submitted by the authors in English.

INTRODUCTION

Short-fiber-reinforced thermoplastic composites have been employed extensively in the plastics industry because of the excellent combination of their mechanical properties, chemical resistance, moderate cost, and recyclability performance. Incorporation of a proper amount (mostly 5 to 20 vol %) of reinforcing fibers into a thermoplastic resin causes significant improvement of tensile strength, modulus, dimensional stability, moisture and corrosion resistance, electrical properties, etc. These properties are closely related not only to the fiber concentration but also to the fiber characteristics such as diameter, length, and distribution.

Production of short-fiber-reinforced polymers is generally carried out via compounding of fibers with a polymer exhibiting a wide range of viscosities to obtain material suitable for various molding procedures. One of the common processing problems is fiber breakage during compounding and molding, a phenomenon that limits the performance of the final product. This negative effect is even more pronounced for recycled composites. It has been shown that the reduction in length might result in a loss of reinforcement efficiency, which is a function of both the total amount of work performed on material and the position of fiber-length distribution relative to the critical fiber length. This quantity was determined by Kelly and Tyson [1] to be between 0.15 and 0.45 mm (depending on the interfacial shear strength). Apparently, in order to enhance composite strength, the average fiber length in a matrix should exceed the critical length as much as possible without interfering with processability. Therefore, it is important to assess the effect of processing variables on the extent of fiber degradation during compounding and processing (extrusion, injection molding) with regard to the subsequent effects on the molded materials.

Many authors have investigated the mechanism of fiber damage (fracture) and the resulting length distribution during or after compounding and extrusion- injection molding [2-24]. It is known that the length reduction is most severe during the first processing stage, i.e., when fiber bundles are being filamentized. The method of fiber incorporation into the polymer melt (addition to molten polymer versus mixing with powdery polymer prior to compounding) was found to have no effect on the final fiber length [6], while polymer viscosity is known to affect the fiber length significantly. Concentration dependences of fiber lengths during various compounding processes suggest that the degradation results from both fiber-fiber and fiber-melt interactions [23, 24].

Fiber fracture due to the shear forces exerted through molten matrix polymer is of special interest because it can be discussed (at least qualitatively) in theoretical terms. In this study, the fiber degradation of fiber-reinforced polymer melts under shear flow in a capillary, as well as their rheological properties after this flow, are investigated on polypropylene-carbon fiber composites prepared in two different types of extruders.

EXPERIMENTAL

Pelletized polypropylene (PP, NOBLEN W101, Sumitomo Chemical Co., Ltd., Japan) served as a matrix polymer. An antioxidant—a mixture of BHT, IRGANOX, and DSTDP—was dry-blended into the polymer to prevent chemical degradation during processing. Used as a reinforcement material, carbon fibers (CF, HTA12000, Toho Beslon Co., Ltd., Japan) were chopped into strands 7 μm in diameter and 3 mm in length.

Weighted amounts of dried polypropylene and chopped strands of carbon fiber (5, 10, l5 and 20 vol %) were mixed thoroughly in a single-screw (screw diameter 19 mm, *L/D* ratio 20, Plasticorder PLV151, Brabender Co., Ltd.) and twin-screw (screw diameter 35 mm, L/D ratio 15, counter-rotation, RT35-2S, Tsukada Juki Co.,

Ltd.) extruders with a screw speed of 25 rpm. The temperature in the compression, melting, and mixing zones was set to 200, 210, and 220°C, respectively. In order to obtain well-dispersed composites via a single-screw extruder, the material was extruded twice through the die. The extrudates were cut into 5-mm-long pellets, which served as feeding material for die swell, flow, and fiber degradation experiments.

Hereinafter, the samples prepared in a single-screw extruder are denoted PP-1 for unfilled PP and CF-1 for carbon-fiber-filled PP. Accordingly, PP-2 represents unfilled, while CF-2 represents filled samples prepared with a twin-screw extruder. The table shows the sample codes, volume fractions of fibers, and initial number-average fiber lengths.

Material characteristics

Code	Fiber volume fraction, Φ_f, %	Number-average fiber length, l_n, mm	Compounding method
PP-1	0	–	Single-screw extruder
CF5-1	5	0.447	
CF10-1	10	0.387	
CF15-1	15	0.292	
CF20-1	20	0.296	
PP-2	0	–	Twin-screw extruder
CF5-2	5	0.334	
CF10-2	10	0.325	
CF15-2	15	0.273	
CF20-2	20	0.225	

At low shear rates the flow properties of two series of CF-filled PP were measured with a cone-plate rheometer (151-S, Nippon Rheology Kiki Co., Ltd., Japan) having a cone/plate radius of 21.5 mm and a cone angle of 4°, while for high shear rates the viscosity data was obtained with a capillary rheometer (Koka-shiki Flow tester, Shimazu Seisakusyo Co., Ltd., Japan). A plane- entrance capillary, 20 mm in length and 1 mm in diameter, was used for the measurements. All the experiments were carried out at 200°C (for low shear rates under a nitrogen atmosphere).

Die swell, which is defined as the ratio of the diameter of the extrudate to that of the capillary (1 mm), was measured as a function of the shear rate and the number of repeated extrusions through the capillary. The fiber length and its distribution were controlled after each extrusion by an ordinary method (burning off matrix polymer in a furnace at 450°C for 4 h, wetting fibers in glycerin and spreading them on a glass plate, where the fiber-length distribution is observed via an optical micrograph). The lengths of at least 500 fibers were

measured carefully on magnified photographs in each experiment. Number-average fiber length l_n and weight-average fiber length l_w were calculated according to the following relations:

$$l_n = \frac{\sum N_i l_i}{\sum N_i} \quad (1)$$

$$l_w = \frac{\sum N_i l_i^2}{\sum N_i l_i} \quad (2)$$

where N_i is the number of fibers and l_i is the fiber length. Thus, l_n is an indicator of the occurrence of short fibers, whereas l_w is an indicator of the occurrence of long fibers.

The effect of repeated extrusion through the capillary at a high shear rate on the cumulative damage of the fibers was investigated.

RESULTS AND DISCUSSION

Rheological Properties of Original CF/PP Samples

The initial breakage of carbon fibers (during mixing) is more pronounced for twin-screw extruder samples than for those from the single-screw extruder under similar processing conditions (table). The length of fibers in the compounded samples depends on their concentration, thus suggesting fiber degradation due to fiber-matrix and fiber-fiber interactions.

Figure 1 demonstrates the relationship between shear viscosity, η, and shear rate, $\dot{\gamma}$, in its low region for the two series of compounded systems, CF/PP-1 (single-screw extruder) and CF/PP-2 (twin-screw extruder), before the extrusion through the capillary (N = 0) and shows clearly different viscosities of both types of systems. Such behavior might be attributed to the different mechanical and thermal-chemical degradation under these varying compounding conditions. Generally, temperature increase due to dissipation of energy is higher for the twin-screw extruder, thereby leading to higher destruction of the PP-2 based samples, as can be seen from Fig. 1. According to the estimation of molecular weight changes from the relation between viscosity and molecular weight (power law for zero-shear viscosity), the molecular weight of PP-2 is approximately 12% lower than that of PP-1. The fiber degradation under low shear rates was found to be negligible.

At this point we will briefly consider the constitutive equation of a three-dimensionally oriented fiber assembly [25, 26]. The assembly is composed of parts *e*, that is, effective fiber elements influenced by the stress of the fiber assembly under deformation, and parts *n* with free ends, therefore being noneffective. Stress tensor, τ_{ij}, of a fiber assembly can be expressed as:

$$\tau_{ij} = \frac{N_f l^2 E \Gamma}{V} \int_0^{2\pi} \int_0^{\pi} \varepsilon_{kl} s_i s_j s_k s_l \Omega(\theta, \psi) \sin\theta d\theta d\psi, \quad (3)$$

where N_f is the total number of fibers per unit volume; l stands for fiber length; V is the volume of fiber assembly; E represents tensile modulus of fiber; ε_{kl} is the strain tensor; s_i, s_j, s_k, s_l are orthogonal coordinates presented by polar coordinates (r, θ, ψ); term Ω(θ, ψ) is the fiber orientation distribution function; and Γ is an effective element fraction, which represents the portion of the effective fiber elements in the total number of

elements.

The effective element fraction Γ can be presented as a function of the number of points, where a fiber is in contact with other fibers, *m*:

$$\Gamma = \left(\frac{m-1}{m+1}\right)^3 \left(\frac{m+5}{m+1}\right). \quad (4)$$

This equation shows that Γ is smaller than the noneffective fiber elements' part (*n*) in the low region of m, while both Γ and *n* approach to 1 when *m* is higher than 100. From the investigation of fiber assembly geometry, the number of contacts is

$$m = \frac{2d(N_f-1)l^2 I}{V}, \quad (5)$$

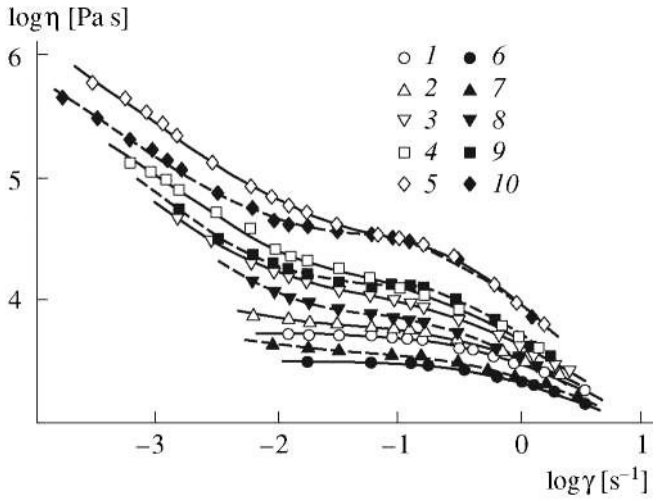

Fig. 1. Relationships between shear viscosities and shear rates of *(1)* PP-1, *(2)* CF5-1, *(3)* CF10-1, *(4)* CF15-1, *(5)* CF20-1, *(6)* PP-2, *(7)* CF5-2, *(8)* CF10-2, *(9)* CF15-2 and *(10)* CF20-2 composites.

where d is fiber diameter and I represents fiber orientation function:

$$I = \int_0^{2\pi}\int_0^{2\pi}\int_0^{2\pi}\int_0^{2\pi} \Omega(\theta,\psi)\Omega(\theta',\psi')|\sin x| \times \sin\theta\sin\theta' d\theta d\theta' d\psi d\psi', \quad (6)$$

$$\sin x = [1 - (\cos\theta\cos\theta' + \sin\theta\sin\theta'\cos(\psi - \psi'))^2]^{1/2}. \quad (7)$$

From Eq. (5), m can be expressed as

$$m = \frac{8}{\pi}\frac{\frac{\pi d^2}{4}N_f l}{V}\frac{l}{d}I. \quad (8)$$

The volume fraction of fiber, Ω_f, and its aspect ratio, a_r, are defined as

$$\Phi_f = \frac{\pi d^2}{4}\frac{N_f l}{V}, \tag{9}$$

$$a_r = \frac{l}{d}. \tag{10}$$

Then,

$$m = \frac{8}{\pi}\frac{\left(\frac{\pi d^2}{4}N_f l\right)}{V}\frac{l}{d}I = \frac{8}{\pi}\Phi_f a_r I\,. \tag{11}$$

Finally, the stress tensor is given as

$$\tau_{ij} = \frac{4}{\pi}\frac{\Phi_f a_r \Gamma E}{d}\int_0^{2\pi}\int_0^{\pi}\varepsilon_{kl}s_i s_j s_k s_l \Omega(\theta,\psi)\sin\theta d\theta d\psi, \tag{12}$$

Both variables, the number of contacting points and the stress tensor, are proportional to the volume fraction of fibers and their aspect ratio. With strain tensor ε_{kl} and fiber orientation distribution function $\Omega(\theta, \psi)$, the shear stress τ_{ij} ($i \neq j$) or shear modulus can be calculated from Eq. (12).

Considering yield stress to be the representative of the critical value of the shear deformation of fiber assembly, we can provide information concerning the relation between yield stress and characteristics of the fiber assembly, such as the volume fraction, fiber orientation, fiber length, or aspect ratio.

Figure 2 gives the relationship between yield stress τ_y estimated from Casson plots and the volume fraction of

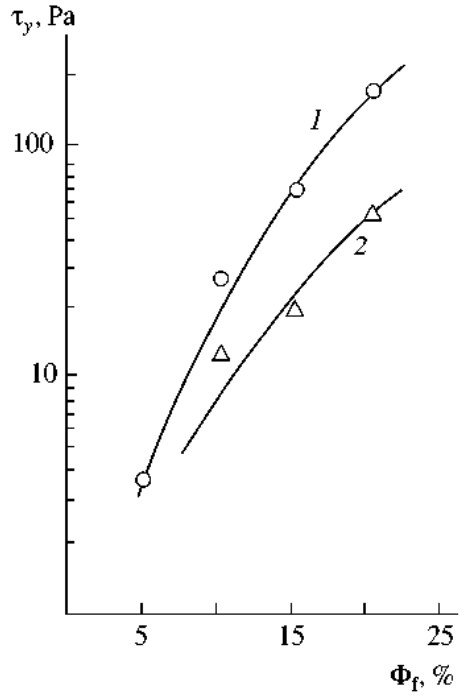

Fig. 2. Shear yield stresses of (1) CF/PP-1 and (2) CF/PP-2 composites as functions of the volume fraction of carbon fiber.

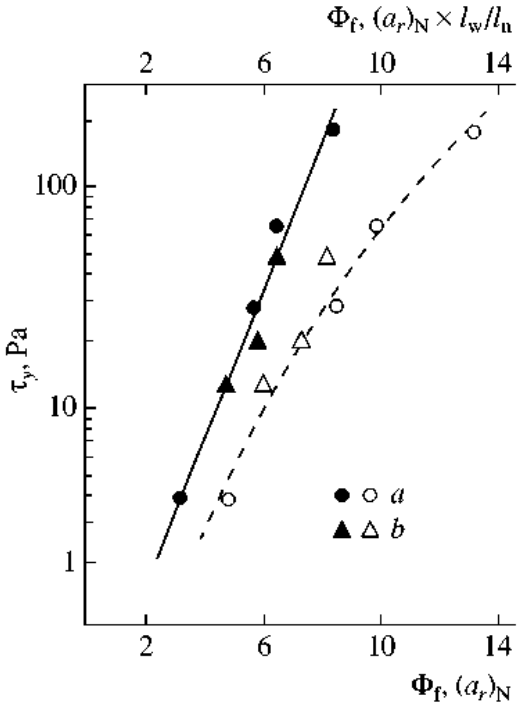

Fig. 3. Shear yield stresses of *(a)* CF/PP-1 and *(b)* CF/PP-2 composites as a function of the modified volume fraction of carbon fibers: by *(1)* number-average aspect ratio $\Phi_f(a_r)_N$ and *(2)* fiber-length ratio $\Phi_f(a_r)_N l_w/l_N(a_r)_N$.

fiber for CF/PP-1 and CF/PP-2 systems in semilogarithmic coordinates. The observed difference in the τ_y–Φ_f plots of the two series might be attributed to different fiber lengths or aspect ratios.

Replotted yield stress data of Fig. 2 as a function of both $\Phi_f(a_r)_N$ and $\Phi_f(a_r)_N l_w/l_N$ are shown in Fig. 3, where $(a_r)_N$ means the number-average aspect ratio. The yield stress' dependence on $(a_r)_N\Phi_f$ in semilogarithmic coordinates gives a single straight line for both CF/PP-1 and CF/PP-2 samples. Then, the yield stress for the samples employed in this study can be described as

$$\tau_y = C\exp[B(a_r)_N\Phi_f]. \qquad (13)$$

The second dependence in Fig. 3 includes the effect of the distribution of the fiber aspect ratio and length. From the nature of l_N and l_w, fiber-length ratio l_w/l_N shows the degree of fiber-length distribution; an increase of this value generally means a broader fiber-length distribution. However, l_w/l_N apparently increases during the fiber-polymer compounding process because the degree of l_N reduction is higher than that of l_w reduction. In this case, the increase of l_w/l_N does not influence yield stress and other rheological properties.

Figure 4 shows apparent shear viscosity as a function of apparent shear rate (high values) measured on a capillary rheometer. Viscosities of both pure PP and its composites with CF follow the power-law model over a wide range of shear rates; however, it is obvious that the viscosity increase with fiber loading is very small in comparison to that observed in the low shear rate region (Fig. 1). Die swells χ of the fiber-filled systems, shown simultaneously in Fig. 4, increase gradually with shear rate (after some plateau) but decrease with fiber loading.

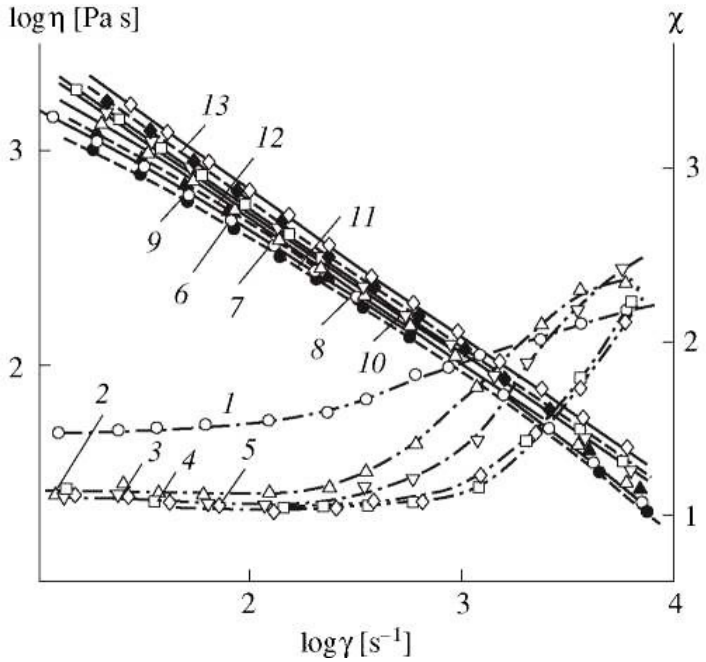

Fig. 4. Die swell of *(1)* PP-1, *(2)* CF5-1, *(3)* CF10-1, *(4)* CF15-1, and *(5)* CF20-1 and apparent viscosities of (6) PP-1, *(7)* CF5-1, (*8*) CF10-1, (9) CF15-1, *(10)* CF20-1, *(11*) PP-2, *(12)* CF5-2, and *(13)* CF20-2 as functions of the apparent shear rate.

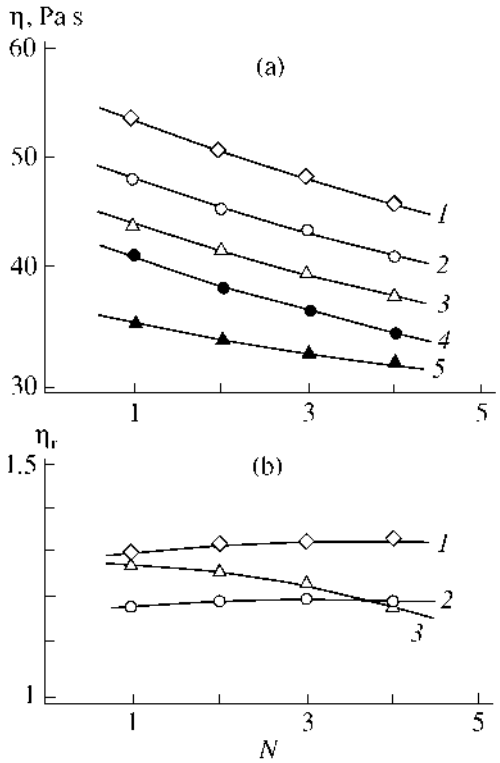

Fig. 5. (a) Apparent viscosities of *(1)* CF10-1, *(2)* CF5-1, (*3*) CF10-2, *(4)* PP-1, and *(5)* PP-2 and (b) relative viscosities of *(1)* CF10-1, *(2)* CF5-1, *(3)* CF10-2 as functions of the number of extrusions through the capillary at a shear rate of 6080 s^{-1}.

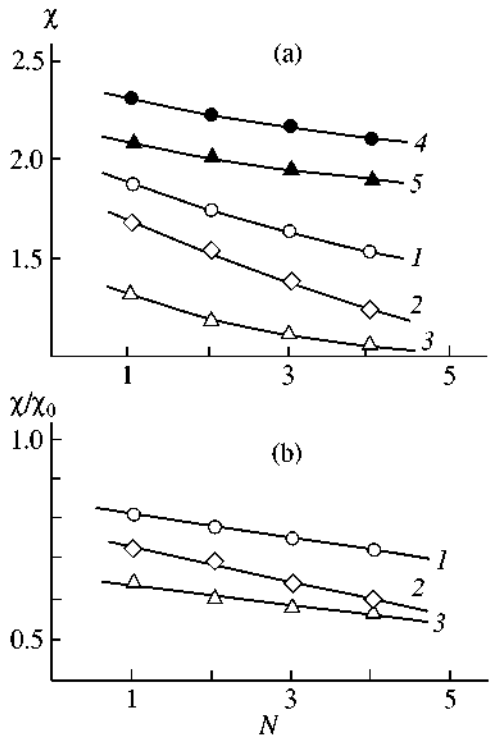

Fig. 6. (a) Die swell of *(1)* PP-1, *(2)* PP-2, *(3)* CF5-1, *(4)* CF10-1, *(5)* CF10-2 and (b) reduced die swell of *(1)* CF5-1, *(2)* CF10-1, and *(3)* CF10-2 as functions of the number of extrusions through the capillary at a shear rate of 6080 s^{-1}.

In general, die swell of fiber-reinforced composites is largely reduced as the content of fibers rises, although the first normal stress difference is reported to increase [4]. At the same time, die swell decreases with a rise in the temperature and a decrease in the screw speed [16]. These phenomena are considered to result from longer fiber degradation as well as the increase of fiber orientation in the flow.

Influence of Multiple Extrusion

Fiber degradation under low shear deformation seems to be negligible if the fiber-length distribution is compared before and after shear-flow experiments carried out on a cone-plate-type rheometer. In contrast, for capillary rheometer experiments both matrix polymer and fiber degradation occurs. Apparent viscosity at a constant shear rate (6080 s^{-1}) as a function of the number of extrusions (Fig. 5a) decreases gradually as extrusion is repeated. The viscosity decrease obtained for the fiber-filled composites is caused mainly by the degradation of matrix polymer. The effect of extrusion-caused fiber degradation or shortening on the decrease of viscosity seems to be relatively small since relative viscosity η_r (the ratio of CF/PP composite viscosity to that of pure PP) does not change distinctively with repeated extrusion, as shown in Fig. 5b.

A similar dependence was studied for die swell χ (Fig. 6a) and reduced die swell χ / χ_0 (Fig. 6b), defined as the ratio of the die swell of a fiber-filled system to that of matrix polymer, which decrease gradually with an increase in the number of extrusion cycles. The decrease of the die swell of fiber-filled systems with the number of passages through the capillary may be caused by the degradation of matrix polymer.

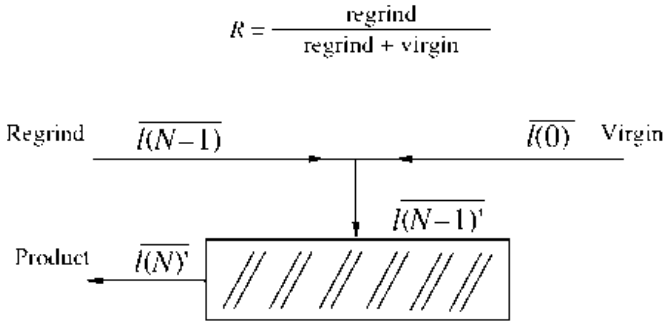

Fig. 7. Schematic of the regrind process.

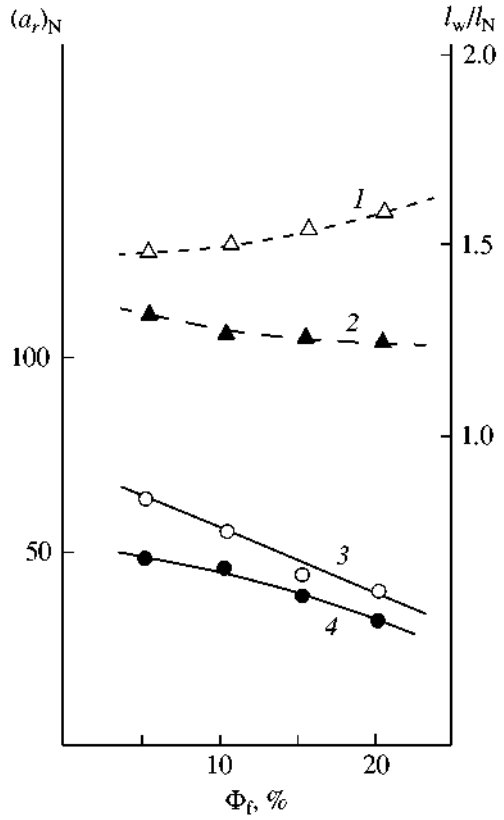

Fig. 8. Fiber-length ratios of *(1)* CF/PP-1 and CF/PP-2 and *(2)* number-average aspect ratios of *(3)* CF/PP-1 and *(4)* CF/PP-2 for virgin samples (not extruded yet) as functions of the volume fraction of carbon fibers.

Fiber Degradation and Change of Fiber Length and Its Distribution

Basic observations concerning the bending behavior of fibers under various flow fields have been made by many researchers, e.g., [8, 17, 27]. For compressive stresses acting along straight fiber, the following equation was proposed for a dilute fiber-suspended system [27]:

$$\tau = \dot{\gamma}\eta = \frac{E_b[\ln(2a_r)-1.75]}{2a_r^4}, \quad (14)$$

where τ represents the critical shear stress for the onset of buckling during laminar flow, $\dot{\gamma}$ is the shear rate, η is viscosity, E_b is the bending modulus of fiber, and a_r stands for aspect ratio of fiber.

Most authors appear to agree that the forces exerted on fibers by molten matrix polymer are the main cause of their degradation. It has been observed that the fiber length is always reduced to a limiting value, which depends on melt viscosity, intensity of shear field, time, and the method of treatment. For example, the regrinding process of glass-fiber-reinforced Nylon 66 was characterized by an exponential decrease of the average fiber length (with an increase in the number of molding cycles) to an asymptotic limit, found to be close to the critical length [2, 6].

The aim of our study is to understand how fiber length can be affected by the mechanical power of the shear-flow field and its repeated application. Under the assumption that the average fiber length after the *N*th regrinding of the molding using the same material is 100%, fiber length can be expressed as [6]

$$\overline{l(N)} = a\exp(-\alpha N) + b = \left[\overline{l(N-1)} - b\right]\exp(-\alpha) + \mathrm{b}, \quad (15)$$

where asymptotic limit b and parameters a and α are strongly affected by molding conditions. Thus, $a + b = \overline{l(0)}$ is the initial average fiber length of the virgin material.

If virgin material is mixed with regrind, the average fiber length for each molding can be estimated as follows: We define regrind ratio R as a function of the regrind portion in the mixed material, while referring to the schematic in Fig. 7. The average fiber length before the *N*th molding, $\overline{l(N-1)'}$ is given as

$$\overline{l(N-1)'} = \overline{l(N-1)}R + \overline{l(0)}(1-R). \quad (16)$$

From Eqs. (15) and (16),

$$\overline{l(N)'} = aR\exp(-N\alpha) + a(1-R)\exp(-\alpha) + b. \quad (17)$$

When R = 1, which corresponds to 100% regrind material, Eq. (17) is reduced to the following form:

$$\overline{l(N)'} = a\exp(-N\alpha) + \mathrm{b}. \quad (18)$$

This is equivalent to Eq. (15).

Since the breakage of fibers is also caused by forces from other fibers, it must depend on the concentration. Figure 8 shows number-average aspect ratio $(a_r)_N$ and fiber-length ratio l_w/l_N of CF/PP-1 and CF/PP-2 in the virgin state (N = 0) as functions of the volume fraction of fiber, Φ_f. Number-average aspect ratio $(a_r)_N$ of both series decreases monotonically with increasing fiber content; however, the fiber-length ratio l_w/l_N, which corresponds to the degree of fiber-length distribution, does not follow such a trend. In contrast, for CF/PP-1, the ratio increases gradually with the fiber content as a possible consequence of the broader fiber-length distribution of CF/PP-1.

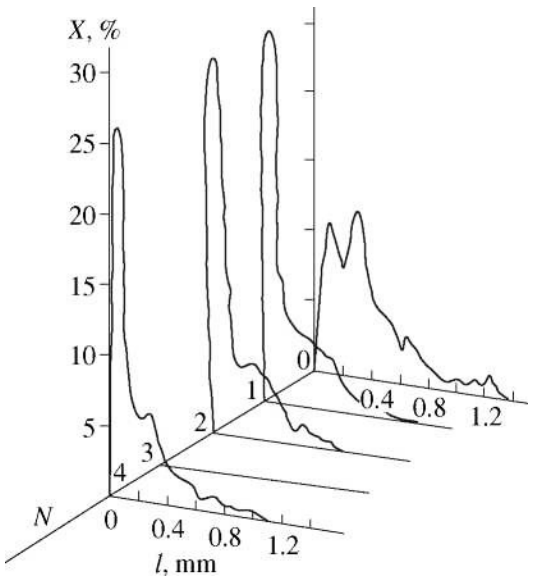

Fig. 9. Fiber-length distribution of the CF10-1 sample at various numbers of extrusion cycles at a shear rate of 6080 s^{-1}. $\Phi_f = 10\%$.

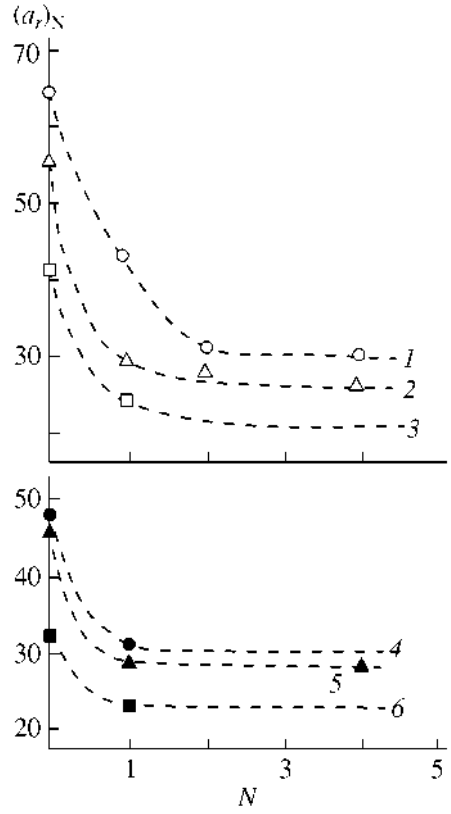

Fig. 10. Number-average aspect ratios of *(1)* CF5-1, *(2)* CF10-1, *(3)* CF20-1, *(4)* CF5-2, *(5)* CF10-2, and *(6)* CF20-2 composites as functions of the number of extrusion cycles at a shear rate of 6080 s^{-1}. The dashed lines represent the same dependence predicted from equation (17) with coefficients *a* equal to (a) 1.9 and (b) 3.1.

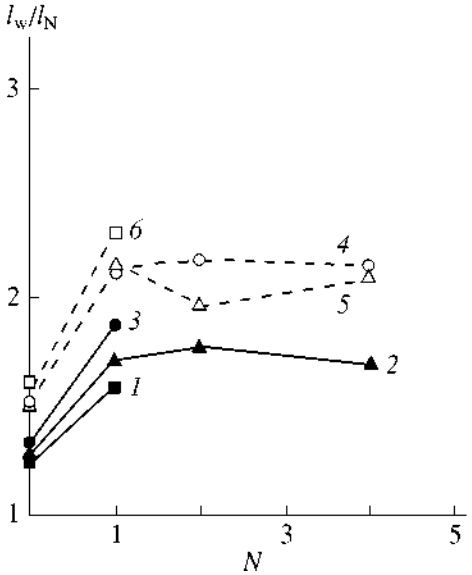

Fig. 11. Fiber-length ratio as a function of the number of extrusions through the capillary at a shear rate of 6080 s^{-1} for *(1)* CF20-2, *(2)* CF10-2, *(3)* CF5-2, *(4)* CF5-1, *(5)* CF10-1, and *(6)* CF20-1 composites.

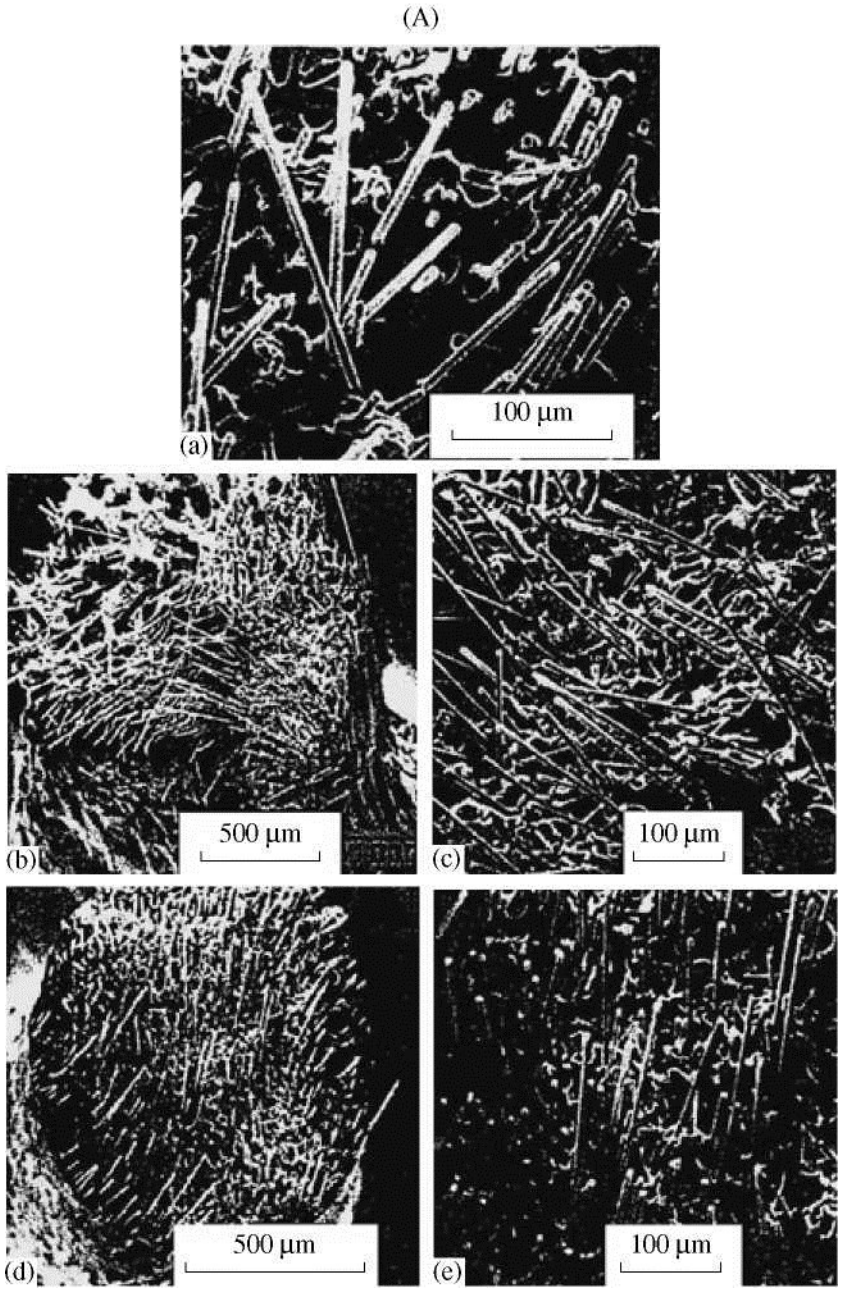

Fig. 12. SEM photographs of the fracture surface of (A) the CF10-1 and (B) CF10-2 samples extruded through the capillary at a shear rate of 6080 s^{-1} after (a) 0, (b, c) 1, and (d, e) 4 repetitions of the extrusion process.

From the observation of fiber-length distribution of each virgin sample with different content of fiber, it was found that the shape of the distribution changes with the content of fiber. Further, the fiber length, in which the curve has a maximum, decreases with rising fiber content, while the length distribution of fibers of CF/PP-2 samples is very different from that of CF/PP-1.

Fiber fracture during processing is generally interpreted in terms of two types of interactions: (i) stresses induced by the flowing melt without any concurrent actions from other fibers and (ii) stresses resulting from

fiber-fiber interactions (collisions, spatial hindrances, friction, etc.). At very low concentrations, the fiber fracture can result only from fiber-melt interactions. As an example, the results obtained for CF10-1, i.e., 10 vol % of carbon fibers, are shown in Fig. 9. The fiber distribution changes after every extrusion through the capillary, and the fibers become remarkably shorter after the first extrusion. All fiber-length distributions were found to be positively skewed. The degree of the skew is related to the amount of work performed on the composite: the larger the amount of work, the smaller the average fiber-length and the shorter the skew tail.

Figure 10 shows number-average aspect ratio $(a_r)_N$ as a function of the number of extrusions N through the

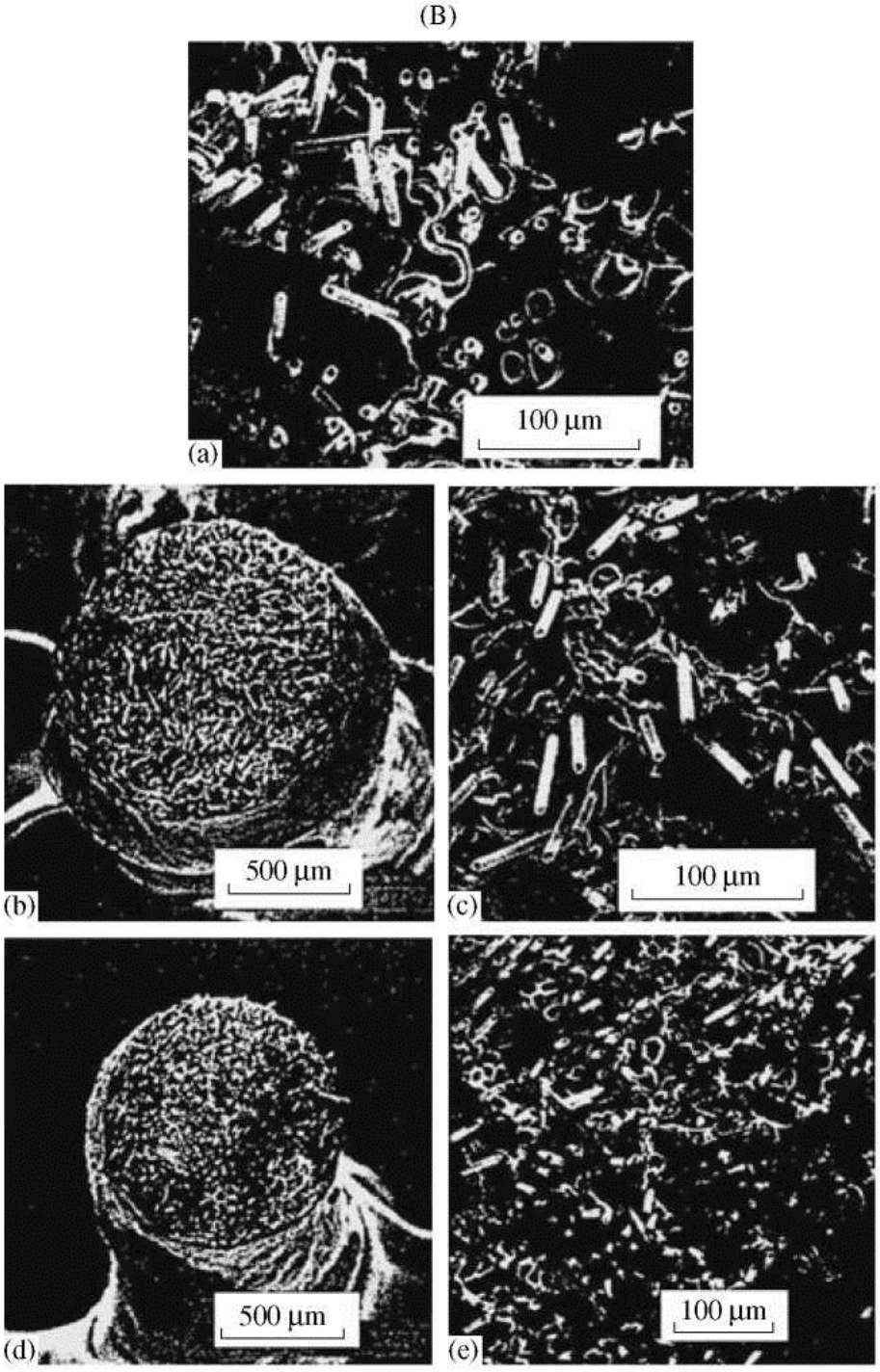

Fig. 12. (Contd.)

capillary at an apparent shear rate of 6080 s^{-1} for (a) CF/PP-1 and (b) CF/PP-2. The experimental points follow the trends represented by the following equation, which was derived from Eq. (15):

$$a_r(N) = l(N)/d = a\exp(-\alpha N) + b\ ,\ a + b = a_r(0), \qquad (19)$$

where parameters a and b are constants determined from the initial fiber-length or aspect ratio of the particular sample and α is the fitting parameter, found to be 1.9 for CFIPP-1 and 3.1 for CFIPP-2 compounds.

It is clear from Fig. 10 that the aspect ratios of all fiber composites decrease abruptly after the first passage through the capillary. The effect of repeated extrusion on the fiber-length ratio as a function of the number of extrusions is depicted in Fig. 11. The fiber-length ratios, corresponding to the degree of the fiber-length distribution, increase abruptly after the first extrusion, while they do not change apparently when extruded repeatedly. As discussed above, such a trend does not indicate an increase of l_w relative to l_N, but reflects a greater decrease of l_N in comparison with that of l_w after extrusion through the capillary.

SEM Observation of Fracture Surfaces

In order to compare fracture surfaces of both PP-1- and PP-2-based composites, SEM photographs (Fig. 12) were taken at various extrusion stages. The upper figures show the virgin samples ($N = 0$), the middle figures depict the situation after the first extrusion ($N = 1$) in different magnification, and the bottom pictures demonstrate the state of the fracture surfaces after the fourth extrusion ($N = 4$). The fiber-length decreases caused by the repeated extrusion, as well as the fiber orientation in the flow direction, can be seen from the micrographs along with a smaller fiber length or aspect ratio of CF10-2 samples in comparison to CF10-1 composites.

CONCLUSIONS

Flow properties of short carbon-fiber-filled polypropylene melts in a wide range of shear rates, as well as fiber degradation during extrusion through a capillary, were investigated.

The yield stresses, representing the critical values of the shear deformation of the fiber assembly, are related to the volume fraction of fibers and the number-average aspect ratio, as shown in Eq. (13).

Under high shear rates (capillary rheometer experiments), both viscosity and die swell of the fiber-filled systems decrease with repeated extrusion, a result that is due to the degradation of the matrix polymer and the reduction of fiber length. The length of fibers decreases with an increase in the number of extrusion cycles, and severe damage of the fibers occurs during the first extrusion, independent of extrusion speed or shear rate.

From these results, it may be concluded that the changes that arise in the fiber lengths or aspect ratios owing to repeated extrusions depend on the initial fiber-length distribution and are independent of the initial fiber lengths or aspect ratios themselves.

ACKNOWLEDGMENTS

We are grateful to the Ministry of Education, Youth, and Sports of the Czech Republic (grant no. MSM 7088352101) for the financial support of this research.

REFERENCES

1. A. Kelly and J. Tyson, J. Mech. Phys. Solids 13, 329 (1965).
2. W. C. Filbert, Jr., SPE J. 25 (65), 65 (1969).
3. K. Stade, Polym. Eng. Sci. 17, 50 (1977).
4. Y. Chan, J. L. White, and Y. Oyanagi, J. Rheol. (N. Y.) 22, 507 (1978).
5. J. M. Lunt and J. B. Shortall, Plast. Rubber Process., September, 108 (1979).
6. H. W. H. Yang, R. Farris, and J. C. W. Chien, J. Appl. Polym. Sci. 23, 3375 (1979).
7. L. Czarnecki and J. L. White, J. Appl. Polym. Sci. 25, 1217 (1980).
8. A. Salinas and J. F. T. Pittman, Polym. Eng. Sci. 21, 23
9. J. B. Shortall and D. Pennington, Plast. Rubber Process. Appl. 2, 33 (1982).
10. R. A. Schweizer, Polym. Plast. Technol. Eng. 18, 81
11. R. Von Turkovich and L. Erwin, Polym. Eng. Sci. 23, 743 (1983).
12. S. Jakopin, Adv. Chem. Ser., 134 (1974).
13. B. Fisa, Polym. Compos. 6, 232 (1985).
14. A. G. Gibson, Plast. Rubber Process. Appl. 5, 95 (1985).
15. D. M. Bigg, Polym. Compos. 6, 20 (1985).
16. W. Y. Chiu and G. D. Shyu, J. Appl. Polym. Sci. 34, 1493 (1987).
17. B. Franzen, C. Klason, J. Kubat, and N. T Kita, Composites 20, 65 (1989).
18. V. B. Gupta, R. K. Mittal, P. K. Sharma, et al., Polym. Compos. 10, 8 (1989).
19. V. B. Gupta, R. K. Mittal, P. K. Sharma, et al., Polym. Compos. 10, 16 (1989).
20. D. Wall, Polym. Compos. 10, 98 (1989).
21. M. A. Ramos and F. A. Belmontes, Polym. Compos. 12, 1 (1991).
22. K. Ramani, D. Bank, and N. Kraemer, Polym. Compos. 16, 258 (1995).
23. P. A. Eriksson, A. C. Albertsson, P. Boydell, et al., Polym. Compos. 17, 823 (1996).
24. P. A. Eriksson, A. C. Albertsson, P. Boydell, et al., Polym. Compos. 17, 830 (1996).
25. K. Yamada and A. Horikawa, J. Text. Eng. Jpn. 36, 51 .
26. K. Yamada, PhD Thesis (Osaka Univ., Osaka, 1986).
27. O. L. Fagacs and S. G. Mason, J. Colloid Sci. 14, 457 (1959).